Localized growth and branching random walks with time correlations

Thomas Gueudré*
Politecnico di Torino, 10129 Torino, Italy
(Received 19 December 2016; revised manuscript received 22 March 2017; published 19 April 2017)

We generalize a model of growth over a disordered environment, to a large class of Itō processes. In particular, we study how the microscopic properties of the noise influence the macroscopic growth rate. The present model can account for growth processes in large dimensions and provides a bed to understand better the tradeoff between exploration and exploitation. An additional mapping to the Schrödinger equation readily provides a set of disorders for which this model can be solved exactly. This mean-field approach exhibits interesting features, such as a freezing transition and an optimal point of growth, which can be studied in detail, and gives yet another explanation for the occurrence of the *Zipf law* in complex, well-connected systems.

DOI: 10.1103/PhysRevE.95.042134

I. INTRODUCTION

Growth is among the most evident properties of complex systems and pervades studies ranging from econometry [1,2] and state policies [3,4] to cell biology [5] and genetics [6]. An outcome either to be sought after (the holy grail of economy) or to be impeded (in tumors and epidemics), it nonetheless remains notoriously difficult to measure and predict [7]. This is partly because, in numerous cases, growth is dynamically shaped by environmental cues, for example when foraging resources [8], balancing a portfolio of assets [9], choosing the next step in a chess game [10], etc. How do populations adapt to their ever-changing environment? How do they tune exploration strategies to cope with uncertainty? Those questions have received constant attention (see Ref. [11] and references therein). The difficulties are particularly stringent in complex systems, where growth is at heart an emergent quantity, the macroscopic result of microscopic entities. Choosing the level of description of the system, and understanding to which extent its conclusions are valid—or, so to say, universal—is a standard conundrum [12]; macroscopic, phenomenological models often disregard crucial factors, such as the uneven repartition of growth among the population. Yet overly detailed models are difficult to manipulate—let alone to solve—brittle and little informative.

In the present work, we study in analytical detail the influence of the environment randomness over the growth rate. To that purpose, we will consider a *branching random walk*: a population $Z_i(t)$ lives on the nodes $\{i\}_{i\in N}$ of a graph and grows under multiplicative noise $\eta(t)$ (see Fig. 1):

$$Z_i(t+dt) = Z_i(t)\exp[\eta_i(t)dt].$$

We will make the only assumption that $\eta(t)$ is an Itō process, equipped with a stationary distribution $Q(\eta)$.

The exploration is implemented by adding a branching mechanism, triggered at random with a small probability $\lambda\, dt$ at each time step dt: when this mechanism is triggered, the population $Z_i(t)$ may diffuse over k sites chosen at random among the whole space:

$$Z_i(t+dt) - Z_i(t) = \frac{D}{k}\sum_{\alpha\in\mathcal{N}_i}[Z_\alpha(t) - Z_i(t)],$$

where $\mathcal{N}_i$ denote the random sets of k sites, different from i (see Fig. 1). To avoid cluttering the notations, we will consider the case $k = 1$ and $D = 1/2$, but our computation is straightforward to generalize. The range of this diffusion is infinite and this model therefore belongs to the mean-field class. This approach is adapted to describe very connected worlds (such as on complete graphs). It is particularly relevant in reinforcement learning, where the most common heuristics to solve the exploration and exploitation dilemma, the ϵ-greedy strategy [11,14,15], is to pick a new strategy at random with probability ϵ. As for now, the question of the optimal ϵ remains fully open [16].

We extend a study first started in Ref. [17], where the above model was solved for a specific Itō process. A crucial ingredient in its analytical treatment comes from the community of spin glasses [13,18]. In a series of works, Derrida and coworkers unravelled a deep connection of the *branching Brownian motion* (see Fig. 1) to the traveling wave solution of the so-called Fisher-Kolmogorov-Petrovsky-Piscounov (FKPP) equation, a nonlinear partial differential equation, most often seen in diffusion-reaction context [19]. This mapping has become a standard tool to tackle the branching Brownian motion [20] and already found numerous applications, in a similar spirit for agent-based models where sharing and harvesting compete [21], but also in fragmentation theory or computer science (see, for example, Refs. [22,23]).

Our major result is first computational, as we present a large class of time-correlated growth models (or equivalently branching random walks) for which analytical expressions can be obtained. Aside from Gittins indices [24], often impossible to compute exactly, the panel of solvable growth models exhibiting the exploration and exploitation dilemma is still sparse. This fact has to be compared with the jungle of existing stochastic processes [25,26], whose enormous development has been triggered by dire modeling needs. The present contribution addresses a similar demand for growth models, apparent in the vast literature about calibrating them onto real datas [27–30]. Second, we will give a detailed description of the rich features of those growth models. Rather striking is the fact that, at low—or zero—diffusion λ, most of the mass is concentrated on few remote sites, that totally dominate the population distribution. The rest of the sites being depleted, the typical growth goes to 0. But it does so quite singularly, and as soon as diffusion is switched on, the population start growing exponentially almost everywhere. Other important aspects of

*gueudre.t@gmail.com

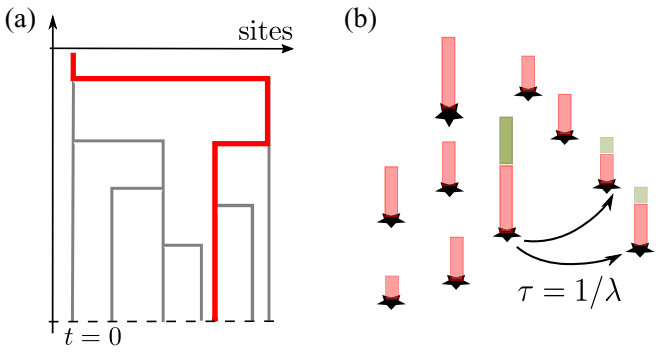

FIG. 1. (Sketch) Illustration of the mean-field model of exploration and exploitation. (a) Polymers on tree (or branching Brownian motion), a model developed in Ref. [13] for tackling the spin-glass problem. (b) Mean-field model of population growth: sites undergo random phase of multiplicative growth or migration. The migration is diffusion-like: sites with large population spread the excess of them (the green block) over a time scale $\tau = 1/\lambda$, while conserving the total number of agents. This amounts to a discrete, infinite-range Laplacian of strength λ.

the present model are the existence of both an optimal and a critical diffusion λ_m and λ_c, with a localization transition. Both points present an interplay that we investigate with the help of the analytical results.

Finally, we mention that these results have interesting implications in other applications of branching random walk that we have not touched upon, such as log-correlated potentials [32,33], Liouville field theory [34], or random matrices [35].

The paper is organized as follows: in Sec. II, we first derive the generalized FKPP equation for Itō processes. In Sec. III, we compute various asymptotic behaviors to bring out the important quantities related to $\eta(t)$. A standard mapping of the Fokker-Planck onto a Schrödinger equation also gives immediately a classification of exactly solvable models [36], and in Sec. IV, we illustrate those findings on two such models, rederiving the results of Ref. [17] in a more direct way. Finally in Sec. V, we discuss the existence and interplay of various features of growth in this class of models, namely the condensation transition, the optimal growth point, and the occurrence of a Zipf law. We also quickly comment on the limitations of the present method.

II. EVOLUTION EQUATION OF THE GROWTH RATE

A. Conventions for the disorder

We will first introduce the details of the disorder, making the assumption that the resources $\eta(x,t)$ obey an Itō equation with time-independent drift and diffusion:

$$d\eta(t) = D_1(\eta)\,dt + \sqrt{2D_2(\eta)}\,dW_t, \tag{1}$$

where W_t is a Brownian process. The probability distribution $P(\eta,t)$ obeys the Fokker-Planck equation (with the Itō prescription):

$$\frac{\partial P(\eta,t)}{\partial t} = -\frac{\partial}{\partial \eta}(D_1(\eta)P(\eta,t)) + \frac{\partial^2}{\partial \eta^2}(D_2(\eta)P(\eta,t)) = \mathcal{L}_0 P(\eta,t), \tag{2}$$

$\mathcal{L}_0$ being the Fokker-Planck operator of the disorder is written. As commonly stated [37], the η dependence of the diffusion $D_2(\eta)$ can be absorbed by a change of variable and we assume it constant in the following. We also assume η to have a stationary distribution:

$$Q(\eta) = \mathcal{N}^{-1}e^{-\Phi(\eta)} \text{ with } \mathcal{N} = \int d\eta e^{-\Phi(\eta)},$$

$$\Phi(\eta) = \log D_2 - \int^{\eta} \frac{D_1(u)}{D_2}du,$$

with natural boundary conditions (or reflecting in case of bounded support). We comment on this hypothesis later in Sec. V. As Φ is defined up to a constant, it can be written as f:

$$\Phi(\eta) = f(\eta)/D_2, \tag{3}$$

$$f(\eta) = -\int^{\eta} D_1(u)du, \tag{4}$$

with f the potential of the process.

Finally, a nonzero mean $\mu = \int \eta Q(\eta)d\eta$ simply adds a constant contribution to the growth rate. We set such mean to 0 and focus on the contribution stemming from the fluctuations of the disorder.

We will especially examine the interplay between exploration and time correlations. To quantify those correlations, it is natural to introduce the—normalized—integrated time correlation function [37]:

$$T = \int_0^{\infty} \frac{K_\eta(t)}{K_\eta(0)}dt,$$

$$K_\eta(t) = \langle \eta(t)\eta(0)\rangle_Q,$$

where $\langle\cdots\rangle_Q$ denotes in the following the average with respect to η. T can be expressed in terms of the coefficients in Eq. (1), as [38]

$$T = \frac{1}{K_\eta(0)}\int_{-\infty}^{\infty}\frac{dx}{D_2(x)Q(x)}\left[\int_{-\infty}^{x} s\,Q(s)\,ds\right]^2. \tag{5}$$

In the following, we will start all our stochastic processes at stationarity, so $K_\eta(0)$ reduces to the variance $\langle\eta^2\rangle_Q$ of $Q(\eta)$.

B. The evolution equation of the growth process

We consider a large number N of sites, each populated by $Z_i(t)$ elements and resources $\eta_i(t)$, $i = 1,\ldots,N$. According to the rules presented in the Introduction, each $Z_i(t)$ evolves as

$$Z_i(t+dt) = \begin{cases} Z_i(t)\exp[\eta_i(t)dt] & \text{prob.} \quad 1-\lambda\,dt \\ \frac{1}{2}(Z_i(t)+Z_j(t)) & \text{prob.} \quad \lambda\,dt, \end{cases} \tag{6}$$

where $j \neq j$ labels a site chosen at random among the rest. There is considerable freedom in choosing the branching process. We stick to the most common Poisson branching, with a fixed rate λ, but the derivation below can be easily generalized (see Ref. [17] for some examples).

Owing to its wide fluctuations, the magnitude of $Z_i(t)$ can be estimated in two ways: picking one realization of the disorder and considering its almost sure behavior (the

quenched setting), or averaging Z_i over all possible realizations of the disorder (the annealed setting). Therefore, central quantities are the *typical* growth rate c_q and the more common *average* growth rate c_a:

$$c_q = \frac{1}{t\,N}\left\langle \sum_j \log Z_j(t) \right\rangle, \tag{7}$$

$$c_a = \frac{1}{t\,N}\sum_j \log\langle Z_j(t)\rangle. \tag{8}$$

The first quantity, although harder to calculate, is more representative of the typical, most likely, growth, and we focus on it, following the approach of Derrida and coworkers [13,39] and Ref. [17] and defining the generating functions, for any i:

$$G_t(x,\eta) := \langle \exp[-e^{-x}Z_i(t)]\delta[\eta_i(t)-\eta]\rangle, \tag{9}$$

$$\hat{G}_t(x) := \int_{-\infty}^{\infty} d\eta\, G_t(x,\eta) = \langle \exp[-e^{-x}Z_i(t)]\rangle, \tag{10}$$

$$G_{t=0}(x,\eta) = \exp(-e^{-x})\,Q(\eta). \tag{11}$$

We assume the disorder initialized at stationarity and $Z_i(t=0)=1$. Due to the temporal persistence of the disorder η, we need to keep track of its value through $G_t(x,\eta)$. Combining the definition Eq. (9) with the evolution Eq. (6) and averaging over the disorder, one obtains the following evolution equation for $G_t(x,\eta)$:

$$\begin{aligned} G_{t+dt}(x,\eta) = {} & (1-\lambda\,dt)\langle \exp[-e^{-x+\eta_i(t)dt}Z_i(t)]\delta[\mathcal{G}\,\eta_i(t)-\eta]\rangle \\ & +\lambda\,dt\,\langle \exp[-e^{-x-\log(2)}Z_i(t)]\delta[\eta_i(t)-\eta]\rangle \\ & \times\langle \exp[-e^{-x-\log(2)}Z_j(t)]\rangle, \end{aligned} \tag{12}$$

with $\mathcal{G}$ the infinitesimal propagator of η_t over an increment of time dt. Expanding the arguments of G_t for small dt:

$$\begin{aligned} \partial_t G_t(x,\eta) = {} & \mathcal{L}_0 G - \eta\partial_x G + \lambda[G_t(x-\log(2),\eta) \\ & \times \hat{G}_t(x-\log(2)) - G_t(x,\eta)], \end{aligned} \tag{13}$$

with $\mathcal{L}_0$ the Fokker-Planck operator given Eq. (2). This partial differential equation seems rather difficult to solve, but should be, under disguise, the equation of a wave traveling along the x direction—although it lacks the diffusion term in x, such as in Ref. [13]. Indeed, looking back at Eq. (10), $\hat{G}_t(x)$ goes from 0 at $x\to-\infty$ to 1 at $x\to+\infty$, and the crossover between 0 and 1 occurs around $\log Z_i(t)$. $\hat{G}_t(x)$ has therefore the structure of a traveling wave. It turns out that its speed of propagation, that we denote c, is directly linked to c_q, the typical growth rate Eq. (7)! This fact can be seen, for example, from the following representation of the logarithm [13]:

$$\begin{aligned} \langle \log Z_j(t)\rangle &= \int_{-\infty}^{\infty} dx\,\langle \exp(-e^{-x}) - \exp(-e^{-x}Z_j(t))\rangle \\ &= \int_{-\infty}^{\infty} dx[\hat{G}_0(x) - \hat{G}_t(x)], \end{aligned}$$

and so from Eq. (7), $c_q \simeq \langle \log Z_j(t)\rangle/t \simeq c$. Therefore, we only need to know the asymptotic speed of the wave obeying Eq. (13), a task much simpler than computing the full solution. Those traveling wave solutions are well-studied and called *pulled fronts* because their speed is slaved to the exponential decay at the front of the wave. The standard procedure to extract the relation between the propagation speed and the frond decay is to linearize the evolution equation by plugging the functional Ansatz [40]:

$$\hat{G}_t(x) \approx 1 - e^{-\gamma(x-ct)} \quad \text{for} \quad x\to\infty, \tag{14}$$

with γ the exponential decay in the wave equation. Then keeping the dominant terms, one extracts the *dispersion relation* $c(\gamma)$. Here, however, we need to formulate an additional Ansatz for the noise variable η. Noting that for $x\to+\infty$,

$$G_t(+\infty,\eta) \sim \langle \delta[\eta_i(t)-\eta]\rangle = Q(\eta), \tag{15}$$

this suggests looking at the following bivariate Ansatz for $G_t(x,\eta)$, with the dependence in x and η factorized [17]:

$$G_t(x,\eta) \simeq Q(\eta) - R(\eta)e^{-\gamma(x-ct)}, \tag{16}$$

under the constraints

$$\int_\eta Q(\eta)d\eta = \int_\eta R(\eta)d\eta = 1. \tag{17}$$

Plugging the above Ansatz Eq. (16) into Eq. (13) and identifying terms of order 1 and terms of order $e^{-\gamma(x-ct)}$, Eq. (13) reduces to the following system:

$$0 = \mathcal{L}_0 Q(\eta), \tag{18}$$

$$\begin{aligned} Rc\gamma = {} & \mathcal{L}_0 R + \gamma\eta R + \lambda(1/2)^\gamma Q \\ & \times \int d\eta R(\eta) + R(\eta)\lambda((1/2)^\gamma - 1). \end{aligned} \tag{19}$$

Equation (18) states that $Q(\eta)$ is the stationary distribution of the process $\eta(t)$, consistently with Eq. (15). The scaling degrees of freedom of both equations are fixed by the normalization contraints Eq. (17). Once Q is known, Eq. (19) is simply an inhomogeneous Sturm Liouville problem, whose operator is very similar to the Fokker-Planck operator of η, aside from the bias $\gamma\,\eta$, intimately related to the decay of the front.

It is convenient to introduce $Q_H(\eta) = \sqrt{Q(\eta)} = \mathcal{N}^{-1/2}\exp(-\Phi(\eta)/2)$. Transforming further $\mathcal{L}_0$ into an hermitian operator is accomplished by the change $R(\eta) = \lambda 2^{-\gamma} Q_H(\eta)S(\eta)$, and multiplying the whole equation by $\sqrt{\mathcal{N}}\exp(\Phi(\eta)/2)$ leaves us with the new system:

$$\mathcal{L}_H S + \gamma\eta S - \hat{\lambda}S(\eta) = -Q_H, \tag{20}$$

$$\hat{\lambda} = \lambda(1-(1/2)^\gamma) + c\gamma, \quad \mathcal{L}_H = e^{\Phi/2}\mathcal{L}_0 e^{-\Phi/2}. \tag{21}$$

Solving this system is standard, and we adopt the Green Function (or resolvent) formalism [41]. We first consider the homogeneous version of Eq. (20):

$$\mathcal{L}_H S + \gamma\eta S + \alpha S = 0, \tag{22}$$

for any real α. As we assume a constant diffusion coefficient D_2, it is instructive to cast Eq. (22) into a Schrödinger form:

$$\tfrac{\partial^2 S}{\partial\eta^2} = V(\eta)S - \tfrac{\alpha}{D_2}S, \tag{23}$$

$$V(\eta) = \frac{D_1(\eta)^2}{4D_2^2} - \frac{D_1(\eta)' + 2\gamma\eta}{2D_2}. \tag{24}$$

This analogy is particularly useful for exploring some exactly solvable models, as we can draw from the wisdom in quantum mechanics, and we will illustrate it through some examples below. The regular Sturm-Liouville theory asserts that solutions of Eq. (22) can be decomposed over the eigenset $\{\alpha_n\}$ and $\{\phi_n\}$, $n \in \mathbb{N}^+$. We will assume from now on that Eq. (22) has at least one bound state solution (in other words, at least α_0 is isolated, at the bottom of the spectrum), the significance of such hypothesis will become clearer later on. We also use the common convention to write the decomposition as a discrete sum:

$$(\mathcal{L}_H + \gamma\eta)\phi_n = -\alpha_n\phi_n, \quad S(\eta) = \sum_n s_n\phi_n(\eta). \tag{25}$$

Plugging it into Eq. (20),

$$\sum_n (-\alpha_n - \hat{\lambda})s_n\phi_n = -Q_H,$$

and because $\{\phi_n\}$ is a complete orthonormal basis,

$$s_n(\alpha_n + \hat{\lambda}) = \langle Q_H|\phi_n\rangle.$$

We can therefore write $S(\eta)$ and $R(\eta)$ decomposed as

$$S(\eta) = \sum_n \frac{\langle Q_H|\phi_n\rangle}{\alpha_n + \hat{\lambda}}\phi_n(\eta),$$

$$R(\eta) = \lambda 2^{-\gamma} \sum_n \frac{\langle Q_H|\phi_n\rangle}{\alpha_n + \hat{\lambda}} Q_H(\eta)\phi_n(\eta).$$

Given proper boundary conditions, one can finally recover $c(\gamma)$ as an implicit equation by enforcing the self-consistent condition $\int d\eta\, R(\eta) = 1$, leading to

$$\frac{2^\gamma}{\lambda} = \sum_n \frac{\langle Q_H|\phi_n\rangle}{\alpha_n + \hat{\lambda}} \int_\eta d\eta\, Q_H(\eta)\phi_n(\eta) = \sum_n \frac{\langle Q_H|\phi_n\rangle^2}{\alpha_n + \hat{\lambda}}. \tag{26}$$

The quantity

$$G_\gamma(z) = \sum_n \frac{\langle \phi_n|\phi_n\rangle}{\alpha_n - z} \tag{27}$$

is known as the resolvent operator, and ϕ_n and α_n are fixed through Eq. (25). $G_0(z)$ corresponds to the Green function of the system with no bias γ, and its lowest eigenvector is precisely $Q_H(\eta)$, of eigenvalue $\alpha_0 = 0$. We can compactly rewrite the above system as

$$\langle Q_H|G_\gamma(\lambda(2^{-\gamma} - 1) - c\,\gamma)|Q_H\rangle = \frac{2^\gamma}{\lambda}. \tag{28}$$

The above formula is the sought-after dispersion relation that allows to extract c_λ as a function of the front decay γ, for any value of the parameter λ, D_1, and D_2 (as our control parameter is λ, we emphasize its effect on $c_\lambda(\gamma)$ with a subscript in all what follows). Remains only to determine how the variable γ is fixed, given the preparation of $G_{t=0}(x,\eta)$. This requires a rather subtle analysis of the behavior of the front decay in traveling wave equations [13], and we recall this analysis in our setup in the following.

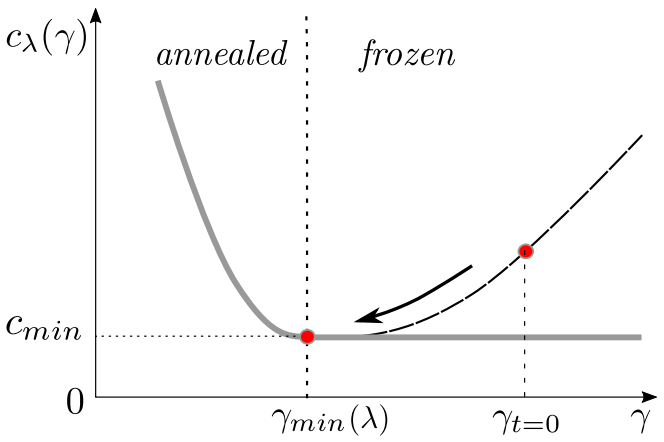

FIG. 2. (Sketch) The growth rate c_λ as a function of γ. Typically, $c_\lambda(\gamma)$ decreases at small γ and increases at large γ. For a front prepared with an initial decay $\gamma_{t=0} < \gamma_{\min}(\lambda)$, the front propagates at $c_\lambda(\gamma_{t=0})$. On the other hand, for a front with $\gamma_{t=0} > \gamma_{\min}(\lambda)$ (the increasing branch of $c_\lambda(\gamma)$), the front will relax toward the minimum, asymptotically propagating at a speed $c_\lambda(\gamma_{\min})$ (the frozen regime).

III. GENERAL RELATIONS BETWEEN GROWTH AND DIFFUSION

A. The selection of the propagation speed

As written, Eq. (28), obtained from linearizing Eq. (13), gives an implicit relation between c_λ and the decay of the front γ, with the details of the noise D_1, D_2 and the diffusion rate λ as parameters. For any value of those parameters, $c_\lambda(\gamma)$ exhibits a minimum (see Fig. 2), whose position $\gamma_{\min}(\lambda)$ depends on the parameters; in particular, it is an increasing function of λ.

The asymptotic value of γ adopted by the front essentially depends on the initial conditions and is prescribed by the *Kolmogorov velocity selection principle* [13,42]: if a traveling wave is prepared at $t = 0$ with a decay $\gamma_{t=0}$ smaller than $\gamma_{\min}(\lambda)$, such decay is maintained and the wave adopts a speed $c_\lambda(\gamma_{t=0})$. On the other hand, if the front is initially prepared with $\gamma_{t=0}$ sharper than $\gamma_{\min}(\lambda)$, its decay relaxes over time towards $\gamma_{\min}(\lambda)$ and the asymptotic speed of the front is fixed to $c_\lambda(\gamma_{\min})$ (see Fig. 2).

In our case, we see from Eq. (11) that the front is always initialized with a decay $\gamma_{t=0} = 1$, so the two branches are separated by the point $\gamma_{\min}(\lambda) = 1$, and we denote by λ_c the critical diffusion rate such that $\gamma_{\min}(\lambda_c) = 1$. Then

(a) If $\gamma_{\min}(\lambda) > 1$ or equivalently $\lambda > \lambda_c$, the propagation of the wave with $\gamma_{t=0} = 1$ is possible: such situation corresponds to the *annealed regime*. Plugging $\gamma = 1$ in Eq. (28) leaves us with $c(\lambda) = c_\lambda(\gamma = 1)$ as a implicit function of the noise and λ. We refer to this portion of the curve as the *annealed branch*.

(b) Instead, if $\gamma_{\min}(\lambda) < 1$ or equivalently $\lambda < \lambda_c$, the front decay broadens toward $\gamma_{\min}(\lambda)$, the *frozen regime* (see Fig. 2). Plugging $\gamma_{\min}(\lambda)$ in Eq. (28) yields $c(\lambda) = c_\lambda[\gamma_{\min}(\lambda)]$. We refer to this portion of the curve as the *quenched branch*.

The typical shape of the whole curve $c(\lambda)$ is shown on the sketch Fig. 3. The junction of the quenched and annealed branches described above occurs at λ_c. Interestingly, the whole curve also has a global maximum at $\lambda_m < \lambda_c$. The remaining

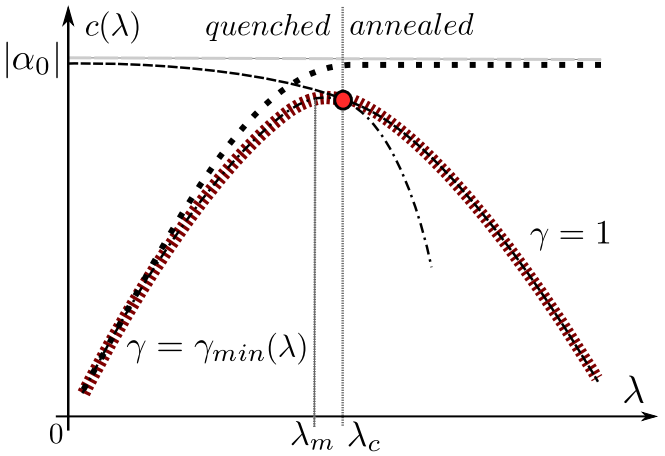

FIG. 3. (Sketch) The growth rate $c(\lambda)$ as a function of λ in log-log plot. Once the critical diffusion rate λ_c is fixed by $\gamma_{\min}(\lambda_c) = 1$, it separates two regimes corresponding to quenched (dashed-dot, $\lambda < \lambda_c$) and annealed (dashed, $\lambda > \lambda_c$) solutions of Eq. (28). Both branches touch at λ_c. In large (red) dashes represent the full curve as dictated by the Kolmogorov velocity selection principle, for a noise with a nonzero correlation time. The white-noise case is also depicted, with black squares, and reaches a plateau equal to $|\alpha_0(\gamma = 1)|$ at λ_c. Typical growth rates exhibit a maximum at a value λ_m, in the quenched phase $\lambda_m < \lambda_c$.

part of the paper will be dedicated to the analysis of this curve for general processes, and illustrated on particular examples.

B. A link with the Stark Effect

To invert Eq. (28) and obtain $c_\lambda(\gamma)$ for any γ, one merely needs to compute the resolvent of Eq. (22), the same as the resolvent of the operator $\mathcal{L}_\mathcal{H}$ with an additional linear bias of amplitude $\gamma\eta$. Green functions are usually difficult to compute. However, this problem is not new and has triggered a large activity in the somewhat unrelated field of Quantum Mechanics (QM), under the name of *Stark effect* [43]: how is a bounded electron perturbed when an electric field is switched on? Of course, the mapping from Itō process to Schrödinger potential may sometimes lead to complicate expressions of $f(\eta)$, but it also provides a way to leverage the computational means developed to tackle the Stark effect. Let us illustrate the similarity of both problems.

We recall from Eq. (21) that $\hat{\lambda} = \lambda(1 - (1/2)^\gamma) + c\gamma$. Note that $\hat{\lambda} > 0$ for any γ, and consider the case γ small. In the left side of Eq. (27), all the terms in the sum, except for $n = 0$, are close to 0, due to the vanishing overlaps. Hence, Eq. (28) reduces to good approximation to

$$\frac{2^\gamma}{\lambda} \simeq \frac{\langle Q_H|\phi_0\rangle^2}{\alpha_0(\gamma) + \hat{\lambda}}, \tag{29}$$

from which we will extract the asymptotics for $\gamma \to 0$. At $\gamma = 0$, excited states all have a higher positive energy. Once γ differs from 0, $\alpha_0(\gamma)$ necessarily becomes negative, a well-known result in QM [43]. As γ goes to 1, the behavior of the series $\{\alpha_n\}_n$ strongly depends on the details of the disorder, and some eigenvalues may cross the y axis, also becoming negative. Therefore, many branches of solutions of Eq. (28) appear, but because we expect $c_\lambda(\gamma)$ continuous, the physical solution remains close to the pole at α_0, and so $c_\lambda(\gamma) < |\alpha_0(\gamma)|$ for any γ.

An important quantity, usually coined the *polarizability* ϵ in quantum mechanics, is defined as

$$\alpha_0(\gamma) = -\epsilon\gamma^2 + O(\gamma^3). \tag{30}$$

(The vanishing of the first order term stems from the fact that the mean of η is set to 0.) The value of ϵ is obtained either using the Rayleigh-Schrödinger theory, or simply expanding the stationary probability distribution $Q(\eta) = |Q_H(\eta)|^2$ in small γ, obtaining for the energy at second order, after some manipulations

$$\epsilon = \frac{1}{D_2}\int_{-\infty}^{\infty}\frac{dx}{Q(x)}\left[\int_{-\infty}^{x} s\,Q(s)ds\right]^2 = \langle\eta^2\rangle_Q\, T, \tag{31}$$

where we have used, for the last line, the general expression for the correlation time defined in Eq. (5). This is an incarnation of the Green-Kubo identity: T is obtained by integrating the temporal two point function $\langle\eta(0)\eta(t)\rangle$, whereas ϵ describes the response to a linear forcing proportional to γ.

In our context, ϵ quantifies the propensity of η to "yield" under the effect of the bias γ. The characteristics of a soft—or very sensitive to the biais—process become rather clear from Eq. (31): it should widely fluctuate or be long time-correlated. We now turn onto a more detailed study of the asymptotics of both annealed and quenched branches.

C. The annealed branch

We first consider the annealed branch, where the decay γ is fixed to 1. Therefore, we denote $c_\lambda(\gamma = 1) = c_a(\lambda)$. Remark that, following the discussion about the selection principle, the annealed branch is not realized in the limit of weak diffusion $\lambda \to 0$. But it provides a useful upper bound for $c_q(\lambda) < c_a(\lambda)$ with

$$c_a(\lambda) = |\alpha_0(\gamma = 1)| - \left(1 - \langle Q_H|\phi_0\rangle^2_{\gamma=1}\right)\frac{\lambda}{2} + O(\lambda^2). \tag{32}$$

The quantity α_0 is the ground-state energy, as defined in Eq. (25). By definition, $\alpha_0(\gamma = 0) = 0$, and $|\alpha_0(\gamma = 1)|$ again measures the energy raise of the ground state under the field $\gamma = 1$, therefore the tendency of the ground state to "polarize." Interestingly, Eq. (32) also provides a compact way to compute the Laplace transform of integrated Markov processes $\langle\exp(\int_0^t \eta(t)dt)\rangle$, an important endeavor in finance [44].

The large λ limit requires to expand the right-hand side of Eq. (28) in inverse powers of λ (to lighten the notations, all the overlaps and eigenvalues in the remaining of this subsection are evaluated at $\gamma = 1$), assuming the overlaps decay exponentially fast at large i:

$$1 = \sum_i \frac{\langle Q_H|\phi_i\rangle^2}{2\alpha_i/\lambda + 1 + 2c(\lambda)/\lambda},$$

$$1 = \sum_i \langle Q_H|\phi_i\rangle^2\left(1 - 2\frac{c(\lambda) + \alpha_i}{\lambda} + \cdots\right).$$

Using together the normalization of Q_H, and the fact that $Q(\eta)$ has zero mean, hence $\langle E\rangle = \sum_i \alpha_i \langle Q_H|\phi_i\rangle^2 = \langle Q_H|\hat{x}|Q_H\rangle = 0$, we obtain

$$c_a(\lambda) = 2\frac{\sum_i \alpha_i^2\langle Q_H|\phi_i\rangle^2}{\lambda} - 4\frac{\sum_i \alpha_i^3\langle Q_H|\phi_i\rangle^2}{\lambda^2} + O(\lambda^{-3}). \tag{33}$$

The coefficient of the dominant decay can be rewritten, using

$$\sum_i \alpha_i^2\langle Q_H|\phi_i\rangle^2 = \int_\eta Q_H(\eta)(\mathcal{L}_H+\eta)^2 Q_H(\eta) = \int_\eta \eta^2 Q_H(\eta)^2 = \langle\eta^2\rangle_Q. \tag{34}$$

Hence the dominant decay is given by the variance of Q. Higher-order terms include higher moments of Q and can be systematically computed.

D. The quenched branch

The quenched branch is more difficult to investigate, as one has also to obtain the location of the minimum $\gamma_{\min}(\lambda)$. We extract the small λ expansion, obtained by considering Eq. (29), under the assumption that both $\gamma_{\min}(\lambda)$ and $c_\lambda(\gamma_{\min})$ go to 0 as $\lambda \to 0$. Plugging Eq. (30) into Eq. (29) and balancing all the terms, we obtain

$$\gamma_{\min}(\lambda) = \sqrt{\frac{\lambda}{\epsilon}} + O(\lambda), \tag{35}$$

$$c_q(\lambda) = 2\sqrt{\epsilon\lambda} + O(\lambda). \tag{36}$$

By expanding to higher order the lowest eigenvalues and overlaps of the resolvent, the approximation can be systematically improved, but the computation quickly becomes tedious.

Note that both asymptotics, large and small λ, depend on the variance and the time correlation of the noise only, a manifestation of universality. One can shed light on those scalings Eqs. (34) and (36) using more hand-waving arguments and the path integral representation:

$$Z(x,t) = \left\langle \exp\left[\int_0^t \eta_{X(s)}(t-s)ds\right]\right\rangle_{\pi_X},$$

where X is a Poisson process over the space of sites, of rate λ and distribution π_X. In the following, we assume that the dominant contribution of the above average stems from a typical behavior of the random walk X, and consider first the small λ case. Over a total time t, λt jumps occur, breaking $\int_0^t \eta_X(s)(t-s)ds$ into λt pieces. Each of those pieces is the integral, over a time $1/\lambda$, of a time T-correlated noise, and so has a typical amplitude of $\sqrt{\langle\eta^2\rangle_Q T/\lambda}$. Deep in the quenched phase, the measure is dominated by the maximum over X, being roughly estimated by

$$\log(Z) \sim \lambda t \times \sqrt{\langle\eta^2\rangle_Q T/\lambda},$$

$$c(\lambda) \simeq \log(Z)/t \sim \sqrt{\langle\eta^2\rangle_Q T\lambda}.$$

The high-λ limit goes along similar same lines and has been presented in Ref. [17] in a different form: first recall that, for the white noise model, the free energy in the annealed phase is fixed to $\langle\eta^2\rangle_Q$. At finite T and large λ, the random walk is so fast, compared with T, that it only sees a frozen disorder on each site, before jumping onto another. Again $\int_0^t \eta_X(s)(t-s)ds$ breaks into λt pieces, but each is now simply the integration, over a time $1/\lambda$, of a frozen random variable η, independently drawn from $Q(\eta)$. Therefore, in this case,

$$\log(Z) \sim \lambda t \times \langle\eta^2\rangle_Q/\lambda^2,$$

$$c(\lambda) \sim \langle\eta^2\rangle_Q/\lambda.$$

IV. PARTICULAR PROCESSES

In this section, we illustrate the computational aspect of the approach, first solving the case of the Ornstein Uhlenbeck by an alternative, but equivalent, route to the one presented in Ref. [17]. We then go onto processes of bounded support, or with varying tails in their stationary distributions. Other solvable examples could be inspired by the literature on Stark effect [45–47].

A. The Ornstein-Uhlenbeck process

The Ornstein-Uhlenbeck (OU) process was the first colored generalization made [17], to our knowledge. This corresponds in QM to the harmonic oscillator, whose solution is completely known. The Fokker-Planck operator and stationary solution are

$$\mathcal{L}_0 = D_2\frac{\partial^2}{\partial\eta^2} + k\frac{\partial}{\partial\eta}\eta,$$

$$f(\eta) = \frac{k\eta^2}{2},$$

$$Q(\eta) = \sqrt{\frac{k}{2\pi D_2}}e^{-\frac{k\eta^2}{2D_2}},$$

$$Q_H(\eta) = \left(\frac{k}{2\pi D_2}\right)^{1/4} e^{-\frac{k\eta^2}{4D_2}}.$$

The problem is equivalent to solving the Schrödinger equation in a potential given by Eq. (24):

$$V(\eta) = \tfrac{k^2\eta^2}{4D_2^2} - \tfrac{k+2\gamma\eta}{2D_2},$$

a tilted harmonic potential. Using $\tilde{\eta} = \sqrt{\frac{k}{2D_2}}\eta - \frac{\sqrt{2D_2}}{k^{3/2}}\gamma$, we reduce it to

$$\frac{\partial^2 S}{\partial\tilde{\eta}^2} = (\tilde{\eta}^2 - \epsilon)S,$$

$$\epsilon = 1 + \frac{2\alpha}{k} + \frac{2D_2\gamma^2}{k^3}. \tag{37}$$

Equation (37) is the celebrated harmonic oscillator, whose propagator goes by the name of the *Mehlerformula*. In the $(\tilde{\eta},\epsilon)$ set of variables:

$$K(\tilde{\eta}_1,\tilde{\eta}_2,t) = \frac{1}{\sqrt{2\pi\sinh(2t)}}\exp\left[\coth(2t)\left(\tilde{\eta}_1^2+\tilde{\eta}_2^2\right)/2 + \operatorname{cosech}(2t)\tilde{\eta}_1\tilde{\eta}_2\right].$$

The resolvent $G_\gamma(z)$ given in Eq. (27) is simply the Laplace transform of the propagator $K(\tilde{\eta}_1,\tilde{\eta}_2,t)$ with respect to t.

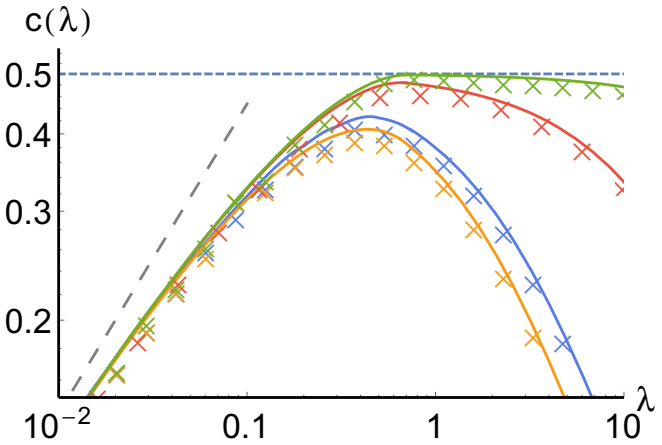

FIG. 4. $c(\lambda)$ as a function of λ for an Ornstein-Uhlenbeck process, with the set of parameters (from top to bottom): $D_2 = 5000, k = 100$; $D_2 = 50, k = 10$; $D_2 = 1, k = \sqrt{2}$; $D_2 = 0.5, k = 1$. The dashed line is the expansion Eq. (36). The scaling have been chosen so that the upper bound $|\alpha_0(\gamma = 0)|$ is fixed to the value 0.5. The numerics are performed on a system of size $N = 10^6$ sites, up to a time $t_{\text{tot}} = 500$, with the discretization time step $dt = 0.001$.

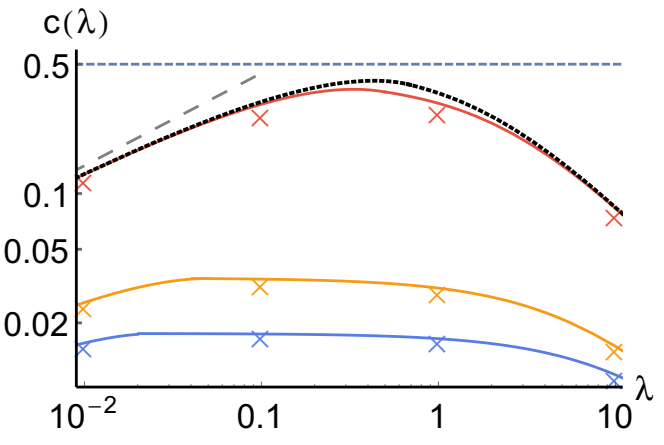

FIG. 5. $c(\lambda)$ as a function of λ for the bounded process, with the set of parameters (from top to bottom): D_2 and a fitted from Eq. (39); $D_2 = 0.5, a = 1$; $D_2 = 1, a = 1$. The dotted line is a fit obtained from the OU process, matching the asymptotic behavior. The dashed line is the expansion Eq. (36). The numerics are performed on a system of size $N = 10^6$ sites, up to a time $t_{\text{tot}} = 500$, with the discretization time step $dt = 0.001$.

Hence, Eq. (28) can be rewritten as

$$\frac{2^\gamma}{\lambda} = \int_{\tilde\eta_1,\tilde\eta_2} d\tilde\eta_1 d\tilde\eta_2 \int_{t=0}^{\infty} dt e^{-\hat\lambda t} K(\tilde\eta_1,\tilde\eta_2,t).$$

Performing both Gaussian integrals in $\tilde\eta_1$ and $\tilde\eta_2$, we are left with

$$\frac{2^\gamma}{\lambda} = \int_0^\infty dt \exp\left[\frac{D_2\gamma^2}{k^3}(e^{-tk}-1) + t\left(\frac{\gamma^2 D_2}{k^2} - \hat\lambda\right)\right], \quad (38)$$

where we recall $\hat\lambda = \lambda[1-(1/2)^\gamma] + c\gamma$. Equation (38) implicitly gives $c_\lambda(\gamma)$, and after selection of the proper branch, the full dependence $c(\lambda)$. Another route (detailed in Appendix A) is to fully diagonalize $\mathcal{L}_{\mathcal{H}}$ and write down the resolvent as an infinite sum. A numerical confirmation of the above result is plotted Fig. 4. The upper bound is $|\alpha_0(\gamma = 1)| = D_2/k^2$, and the set of parameters in Fig. 4 has been chosen so that this upper bound is fixed to $1/2$. As $T = 1/k$ tends to 0 (the white noise limit), $c(\lambda)$ saturates at the plateau $c(\lambda) = |\alpha_0(\gamma = 1)|$ in the annealed phase. This limit is singular, however, as for any small $T > 0$, $c(\lambda)$ decays as λ^{-1}.

B. The bounded noise

Another case of common interest, especially in condensed matter, is the noise of bounded support. It corresponds to a particle in an infinite well, submitted to a uniform electric field, and is again solvable [48], although we end up with a set of transcendental equations.

To simplify slightly the analysis, we set $V(\eta)$ to be a square infinite well, which translates into a bounded but rather contrived Itō process. At $\gamma = 0$, we have

$$V_0(\eta) = -\frac{\pi^2}{4a^2} \text{for } |\eta| < a,$$
$$f(\eta) = -2D_2 \ln\left[\cos\left(\frac{\pi\eta}{2a}\right)\right],$$
$$Q(\eta) = a^{-1}\cos^2\left(\frac{\pi\eta}{2a}\right),$$
$$Q_H(\eta) = a^{-1/2}\cos\left(\frac{\pi\eta}{2a}\right).$$

The eigenset is simply made of Airy functions. The potential with bias is $V(\eta) = -\pi^2/(4a^2) - \gamma\eta/D_2$ and after the change of variables,

$$\tilde\eta = -\left(\frac{\gamma}{D_2}\right)^{1/3}\left(\eta + \frac{\alpha}{\gamma} + \frac{\pi^2 D_2}{4a^2\gamma}\right),$$

we obtain the following eigenbasis, with their according boundary conditions:

$$\phi_n(\eta) = a_n Ai(\tilde\eta) + b_n Bi(\tilde\eta),$$
$$\tilde\eta^b_\pm = -\left(\frac{\gamma}{D_2}\right)^{1/3}\left(\pm a + \frac{\alpha}{\gamma} + \frac{\pi^2 D_2}{4a^2\gamma}\right),$$
$$Ai(\tilde\eta^b_+)Bi(\tilde\eta^b_-) = Ai(\tilde\eta^b_-)Bi(\tilde\eta^b_+).$$

The discrete eigenvalues $\{\alpha_n\}_n$ are solutions of the above transcendental equation. Once this discrete set of eigenvalues is determined, a_n and b_n can be fixed so that the set ϕ_n is normalized and obeys the boundary conditions. We compute the first $N = 10$ terms of the resolvent as an estimate. c as a function of γ is plotted in Fig. 5 and compared with numerical simulations. Once again, the agreement is excellent. In Fig. 5, we also have compared this bounded process with an Ornstein-Uhlenbeck one, matching both T and $\langle\eta^2\rangle$, which

reads

$$\langle \eta^2 \rangle_Q = \frac{a^2(1-6/\pi^2)}{3} = \frac{1}{2},$$
$$T = \frac{a^2(15/\pi^2-1)}{D_2(\pi^2-6)} = 1. \tag{39}$$

Both curves are quite similar, the largest deviation occurs around the freezing transition. It emphasizes the difficulty of choosing a faithful modeling of systems that sit around λ_c.

C. The role of the tails

Growth processes can be seen as extremal in some sense: their statistics are dominated by those space-time paths that manage to collect the largest amount of resources. Inspired by the theory of extreme statistics, one would expect the tails of $Q(\eta)$ to play a prevalent role. The asymptotics mentioned in Sec. III only depend on $\langle \eta^2 \rangle_Q$ and T. To analyze the effects of the tail of $D_1(\eta)$ on T, for example, we define the family distribution Q_μ obtained from $D_1(\eta) \sim \text{sign}(\eta)\,|\eta|^\mu$, such that D_2 and $\langle \eta^2 \rangle_{Q_\mu}$ are normalized to 1. This family smoothly interpolates from the harmonic potential $\mu = 1$ to the infinite well $\mu = \infty$. We then compute $\epsilon(\mu)$ from Eq. (31) using the expression of Q_μ. It turns out that $\epsilon(\mu)$ has a minimum at $\mu = 1$ [the case of the OU process $\epsilon(1) = 1$] and tends to 6/5 at infinity (the process with a uniform stationary distribution and unit variance). The conclusion is that, *at fixed variance*, thinner tails yield an enhanced growth. Although somewhat conterintuitive, it can be traced to the flatter nature of the potential $\Phi(\eta)$ at large μ, when η is close to 0, increasing the polarizability of η.

The perturbative results in the range $\mu \in (0,1)$ have to be taken with a grain of salt, as the perturbation becomes singular and requires a more elaborate treatment [49]. For example, at $\mu = 0$, the process has a Laplace stationary distribution, for which an exact solution exists and one can show that the energy gap between α_0 and the rest of the spectrum vanishes even at small γ. We return to it later, when examining the limitations of this spectral approach.

V. DISCUSSION

The previous exactly solvable cases and the expansions make all the more obvious the existence—and robustness—of both a freezing transition point λ_c, and a maximum at λ_m in the growth rate. At diffusion low enough, the total population is not a self-averaging quantity, and so $c_q < c_a$. The gap between c_q and c_a is due to heavy tails and strong correlations between the $Z_i(t)$. Those factors grow as diffusion decreases, favoring condensation onto few sites. At $\lambda = 0$, Z_i merely reduces to the exponential of $\int_t dt\,\eta(t)$, the integrated Itō process: $\log Z$ is essentially a Gaussian of zero average and growing variance $\langle \eta^2 \rangle T t$, and Z, a log-normal, heavy-tailed distribution. Equation (36) illustrates particularly well the striking effect of diffusion over the typical growth mentioned in the Introduction. Indeed, $c_q(\lambda)$ goes to 0 as $c_q(\lambda) \sim \sqrt{\lambda}$ and so is not derivable in 0 with respect to λ. It is due to the peculiar repartition of the population: at $\lambda \simeq 0$, the total mass is concentrated on very few islands, a phenomenon called *intermittency* [31]. The presence of a diffusion, be it very small, greatly alleviates such condensation by spreading the population over the rest of the system. This tremendous effect of sharing is also observed for models in Euclidian space [31].

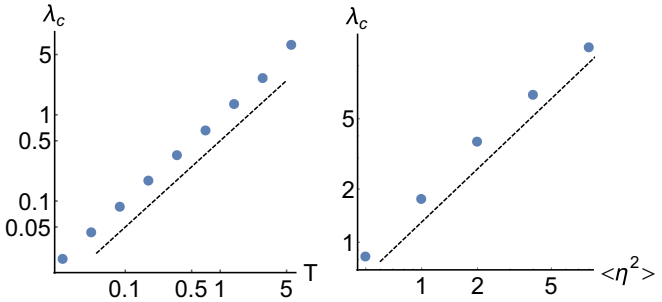

FIG. 6. Scaling of λ_c for the OU process (left) Scaling of λ_c with T, and $\langle \eta^2 \rangle = 1/\sqrt{2}$. (Right) Scaling of λ_c with $\langle \eta^2 \rangle$, and $T = 1.0$. Both dashed lines are guidelines of unit slopes.

There seems to be no close formula neither for the value λ_m at which the freezing transition occurs, nor for the point of optimal growth λ_c. Nonetheless, for any process η, the annealed branch $c_a(\lambda)$ is monotonically decreasing with λ (see Appendix B for a proof), and $c_a(0) = |\alpha_0| \simeq \epsilon$. Assuming the quenched branch is differentiable, we deduce that necessarily $\lambda_m \leqslant \lambda_c$, with equality in the limiting case of white noise. The fact that the optimum always lays in the quenched phase is intriguing, and reminiscent of the Zipf law, a very general attempt to explain the predominance of power-laws in natural systems. The present case falls in the category of *highly optimized tolerance* [50]; when optimized, complex systems have a tendency to develop algebraic tails and experimental studies have shown that they are found close from the optimal point [30]. Given that λ_m and λ_c are not far, it also shows how systems poised at optimality could look critical [51,52].

A rough estimation of the position of λ_c (or λ_m) is obtained by balancing the asymptotics with the upper bound $c_a(\lambda = 0)$, leading to

$$\lambda_c \sim \lambda_m \sim \langle \eta^2 \rangle \times T. \tag{40}$$

In Fig. 6, we tested its validity by numerically solving Eq. (38) for the specific OU process, fixing either $\langle \eta^2 \rangle$ or T. It is also possible to investigate the behavior of λ_m and λ_c close to the white noise limit $T \to 0$, at fixed $\epsilon = 1/2$ (the case presented in Fig. 4). A tedious expansion at small T from Eq. (38) yields both $\lambda_c(T) \simeq \frac{2\epsilon}{\log 4 + T\epsilon(1-\log 2)}$ [$\lambda_c(0) = 0.7213...$] and the fact that the gap $\lambda_c - \lambda_m$ grows linearly with T, with a complicated prefactor that we do not report. Figure 7 numerically confirms the expansion of the gap at small T. In the regime of widely fluctuating noises $T \ll \langle \eta^2 \rangle$, $\lambda_m \simeq \lambda_c$ and a large plateau in $c(\lambda)$ develops around those transition points: the diffusion is still small enough for the noise to be seen as quasiwhite. This suggests that optimal growth is more robust in a wildly varying environment, a rather surprising finding.

On a more practical side, it is often difficult to characterize the properties of the miscrocopic noise $\eta(t)$, and only macroscopic observables are measured. Such situations are common occurrences in biology, for example, where concentrations of proteins or bacteria are much easier to obtain than levels of mRNA or nutrients they harvest. Within the present class of growth models, $\langle \eta^2 \rangle_Q$ and T can be extracted from both

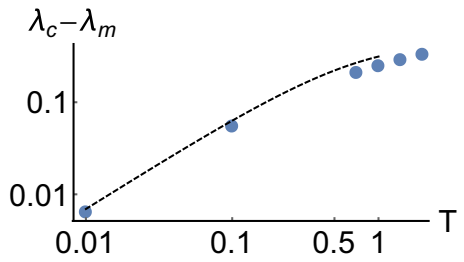

FIG. 7. Scaling of the difference $\lambda_c - \lambda_m$ for the OU process. We have fixed $\epsilon = \frac{D_2}{k^2} = \frac{1}{2}$. The blue dots are the result of the numerical solution of Eq. (38) for specific values of D_2 and $k = 1/T$, while the black dashed line is a small T expansion: $\lambda_c - \lambda_m$ widens linearly with T, close to $T = 0$.

small and large λ (assuming λ is a control parameter of the experiment). Those two values, the most salient features of η, are enough to fit one of the solvable models onto the experience at hand and estimate λ_m and λ_c. We believe the mechanisms presented above to be of more general scope and investigating both the interplay between λ_m and λ_c, as well as their presence in other, non-mean-field growth models, would be a worthy subject of investigation.

To conclude, we will comment on some limitations. The original case made in Ref. [13], and most of the subsequent literature, concerns the pure white noise (also called *branching Brownian motion*). Its evolution cannot be cast into a well-defined Itō equation, but may be obtained as a rather singular limit with $T \to 0$. On the other hand, Itō processes with no stationary distribution $Q(\eta)$—such as the Brownian motion—fall out of the present analysis. Yet we expect them to have no freezing transition: the wandering of those processes is so important that few branches of the tree, if not a single one, should always dominate the statistics. A more precise study would also be welcomed.

The requirement of at least one isolated state at the bottom of the spectrum is a more subtle issue. In principle, such restriction is not necessary, although one would have to tackle the continuous part of the spectrum describing the extended states. The process with the stationary Laplace distribution $Q(\eta) \sim \exp(-|x|)$ is an enlightening example. It translates as a Dirac potential $V(\eta) \sim \delta(\eta)$ in Eq. (24). It is known that a particle in such a narrow potential, and also submitted to an electric field, has no bound state, even for γ infinitesimally small (see Ref. [53] and Appendix C for more details). Therefore, the resolvent has no simple pole, and the expansions presented in Sec. III are not valid anymore. One has to integrate over the branch cut of G_γ, which extends over the whole real axis and regularize it with an ϵ-prescription. While one can write down such equation (see Appendix C), the resulting integrand involves complex, oscillating terms that are very difficult to tackle numerically. In models of the same flavor (such as the random energy model [54,55] or the parabolic Anderson model [56,57]), distributions with such exponential decay lay at the boundary between two different universality classes, and we surmise that the disappearance of the lowest-bound state might have a deeper, statistical, meaning. Enlarging the present derivation to disorders with stretched exponential or even power-law tails, would however require a different approach.

VI. CONCLUSION

In the present work, we have developed a mean-field approach to growth models with temporally correlated disorder. We extended the scope of the well-known traveling wave equation approach, building on work done in Ref. [17]. This method allows for a detailed analysis for a general Itō process and even leads to exact formulas of growth rates for a variety of disorders. We gave three examples, with Gaussian, uniform, or Laplace stationary distributions. It unveils universal features in growth from microscopic details, in particular in the small and large diffusion regimes. This suggests a methodology to fit such models on experimental data. The mean-field computation presents both an optimal growth point and a distinct freezing transition, features that have been also observed in many finite-dimension models. In the present case, the optimal growth always lays in the quenched phase but a more detailed study of the statistics of Z_i is dearly needed and should be possible along the lines of Ref. [13].

To match the numerous directions more phenomenological approaches of growth have taken, we suggest possible extensions of the present study. We wonder how to extend the analysis to heavy-tailed disorders, as they are now recognized as crucial ingredients of the large sensitivity of growth to environmental, financial, or economic shocks [50]. On the same side, the effect of nonstationary environments, adding a temporal dependence to the Itō equation itself, would further our understanding of delayed effects also commonly observed, such as population momentum [58].

Finally, we return to the primary motivations of the "polymers on tree," a spin-glass toy model, and surmise our analysis could be made as rigorous as the original, white noise case [20], an important step toward a theory of such processes. Nonetheless, those models are often treated with the replica tool, a very different and general approach, up to now limited to white-noise disorder. A better understanding of the above derivation in the language of replicas might open many other disordered systems to colored disorder.

ACKNOWLEDGMENTS

We thank Alexander Dobrinevsky and Jean-Philippe Bouchaud for starting this line of thought and many stimulating discussions. We thank two anonymous referees for numerous suggestions.

APPENDIX A: AN ALTERNATIVE SOLUTION OF THE OU PROCESS

Another possibility [17] to solve the OU noise model is to write down the eigenvectors and eigenvalues of the harmonic oscillator and leave the implicit equation as a sum. The normalized eigenbasis is built over the Hermite functions and given by

$$\alpha_n = kn - \frac{\gamma^2 D_2}{k^2}, n \geqslant 0,$$

$$\phi_n = \left(2^n n! \sqrt{\frac{2D_2\pi}{k}}\right)^{-1/2} e^{-\tilde{\eta}^2/2} H_n(\tilde{\eta}),$$

with H_n the Hermite polynomials. Remains to compute the projection of the eigenvectors over Q_H:

$$\langle Q_H|\phi_n\rangle^2 = \frac{1}{n!}\left(\frac{D_2\gamma^2}{k^3}\right)^n e^{-D_2\gamma^2/k^3}.$$

Plugging this expression into Eq. (28) finally leads to an implicit expression for the curve $c(\gamma)$:

$$\frac{2^\gamma}{\lambda} = e^{-D_2\gamma^2/k^3}\sum_{n=0}^{\infty}\frac{(D_2\gamma^2/k^3)^n}{n!(kn-\gamma^2 D_2/k^2-\hat{\lambda})}. \tag{A1}$$

It gives back the result from Ref. [17] with the convention $D_2 = \sigma^2/2\tau^2$ and $k = 1/\tau$.

APPENDIX B: MONOTONOUS DECAY OF THE ANNEALED BRANCH

Here we show that the annealed branch $c_a(\lambda)$, according to Eq. (28), is necessarily a decreasing function of λ. Let us first recall Eq. (28) in the annealed regime $\gamma = 1$,

$$\frac{2}{\lambda} = \sum_{n\geqslant 0}\frac{\langle Q_H|\phi_n\rangle^2}{\alpha_n+\lambda/2+c(\lambda)}, \tag{B1}$$

and derive it with respect to λ:

$$\frac{2}{\lambda^2} = \left(\frac{1}{2}+\frac{\partial c}{\partial\lambda}\right)\sum_{n\geqslant 0}\frac{\langle Q_H|\phi_n\rangle^2}{[\alpha_n+\lambda/2+c(\lambda)]^2}.$$

Substituting the left-hand side with Eq. (B1), we are left with

$$2\frac{\partial c}{\partial\lambda}\sum_{n\geqslant 0}\frac{\langle Q_H|\phi_n\rangle^2}{(\alpha_n+\lambda/2+c(\lambda))^2} = \left[\sum_{n\geqslant 0}\frac{\langle Q_H|\phi_n\rangle^2}{\alpha_n+\lambda/2+c(\lambda)}\right]^2 - \sum_{n\geqslant 0}\frac{\langle Q_H|\phi_n\rangle^2}{[\alpha_n+\lambda/2+c(\lambda)]^2}.$$

But using the Cauchy-Schwart inequality over the first term of the right-hand side:

$$\begin{aligned}&\left(\sum_{n\geqslant 0}\frac{\langle Q_H|\phi_n\rangle^2}{\alpha_n+\lambda/2+c(\lambda)}\right)^2\\ &= \left(\sum_{n\geqslant 0}\langle Q_H|\phi_n\rangle\times\frac{\langle Q_H|\phi_n\rangle}{\alpha_n+\lambda/2+c(\lambda)}\right)^2\\ &\leqslant \left(\sum_n\langle Q_H|\phi_n\rangle^2\right)\left(\sum_n\frac{\langle Q_H|\phi_n\rangle^2}{[\alpha_n+\lambda/2+c(\lambda)]^2}\right)\\ &\leqslant \sum_n\frac{\langle Q_H|\phi_n\rangle^2}{[\alpha_n+\lambda/2+c(\lambda)]^2},\end{aligned}$$

using the fact that

$$\sum_n\langle Q_H|\phi_n\rangle^2 = ||Q_H||_2^2 = \frac{1}{\mathcal{N}}\int_\eta d\eta\,\exp[-\Phi(\eta)] = 1,$$

and so

$$\frac{\partial c(\lambda)}{\partial\lambda}\leqslant 0. \tag{B2}$$

APPENDIX C: THE EXPONENTIAL MODEL

The process with a Laplace stationary distribution represents a singular case in this class of models. It follows

$$\begin{aligned}V(\eta) &= \frac{k^2}{4D_2^3}-\frac{k}{D_2}\delta(\eta) = A - B\delta(\eta),\\ f(\eta) &= k|x|,\\ Q(\eta) &= \frac{k}{2D_2}\exp\left(-\frac{k}{D_2}|x|\right),\\ Q_H(\eta) &= \sqrt{\frac{k}{2D_2}}\exp\left(-\frac{k}{2D_2}|x|\right).\end{aligned}$$

For δ potentials, the Dyson equation can be solved exactly in coordinate representation, and gives the Green function G_γ as a function of the well-known Green function, noted G_0, for the free particle under an electric field [53]:

$$\begin{aligned}G_\gamma(x,y;z) &= G_0(x,y;z)+\frac{B\times G_0(x,0;z)G_0(0,y;z)}{1-B\times G_0(0,0;z)},\\ G_0(x,y;z) &= -i(2\pi i)^{-1/2}\int_0^\infty t^{-1/2}\\ &\quad\times\exp\left[i\left(zt+\frac{(x+y)\gamma t}{2D_2}-\frac{\gamma^2t^3}{24D_2^2}\right)\right]dt.\end{aligned} \tag{C1}$$

Equation (C1) readily shows that no bound state survives to the electric field in a Dirac potential. Equation (28) regularized by the addition of a small imaginary part $\hat{\lambda}\to\hat{\lambda}+i\epsilon$, reduces to (setting $D_2 = 1$ for simplicity):

$$\int_0^\infty dt\,\frac{8e^{i\hat{\lambda}\sqrt{t}}k^3}{(k^2+t\gamma^2)^2}\left(e^{it^{5/2}\gamma^2/24}-e^{i\hat{\lambda}\sqrt{t}}k\right)^{-1} = \frac{2^\gamma}{\lambda}.$$

Although the above equation should lead to the growth rate, the appearance of oscillating terms makes it unsuitable for numerical estimations, and we have been unable to confirm its validity.

[1] G. M. Grossman and E. Helpman, *Innovation and Growth in the Global Economy* (MIT Press, Cambridge, MA, 1993).
[2] D. V. Cavalcanti, V. Tiago, K. Mohaddes, and M. Raissi, J. Appl. Econ. **30**, 857 (2015).
[3] J.-P. Bouchaud, J. Stat. Mech. (2015) P11011.
[4] A. Fatás and I. Mihov, Rev. Econ. Stat. **95**, 362 (2013).
[5] J. Monod, Ann. Rev. Microbiol. **3**, 371 (1949).
[6] É. Brunet and B. Derrida, Philos. Mag. **92**, 255 (2012).

[7] N. N. Taleb, *The Black Swan: The Impact of the Highly Improbable* (Random House, New York, 2007).

[8] M. Chupeau, O. Benichou, and S. Redner, Phys. Rev. E **95**, 012157 (2017).

[9] J.-P. Bouchaud and M. Potters, *Theory of Financial Risk and Derivative Pricing: From Statistical Physics to Risk Management* (Cambridge University Press, Cambridge, 2003).

[10] M. Lai, arXiv:1509.01549 (2015).

[11] J. D. Cohen, S. M. McClure, and J. Y. Angela, Philos. Trans. R. Soc. London B **362**, 933 (2007).

[12] A. Vespignani, Nat. Phys. **8**, 32 (2012).

[13] B. Derrida and H. Spohn, J. Stat. Phys. **51**, 817 (1988).

[14] R. S. Sutton and A. G. Barto, *Reinforcement Learning: An Introduction* (MIT Press, Cambridge, MA, 1998), Vol. 1.

[15] S. C. Pratt and D. J. Sumpter, Proc. Natl. Acad. Sci. USA **103**, 15906 (2006).

[16] M. Tokic, in *Annual Conference on Artificial Intelligence* (Springer, Berlin, 2010), pp. 203–210.

[17] T. Gueudré, A. Dobrinevski, and J.-P. Bouchaud, Phys. Rev. Lett. **112**, 050602 (2014).

[18] É. Brunet and B. Derrida, J. Stat. Phys. **143**, 420 (2011).

[19] P. Grindrod, *The Theory and Applications of Reaction-Diffusion Equations: Patterns and Waves* (Clarendon Press, London, 1996).

[20] L.-P. Arguin, A. Bovier, and N. Kistler, Probab. Theory Relat. Fields **157**, 535 (2013).

[21] S. N. Majumdar and P. L. Krapivsky, Phys. Rev. E **63**, 045101 (2001).

[22] P. L. Krapivsky and S. N. Majumdar, Phys. Rev. Lett. **85**, 5492 (2000).

[23] S. N. Majumdar and P. L. Krapivsky, Phys. Rev. E **65**, 036127 (2002).

[24] J. C. Gittins and D. M. Jones, in *Progress in Statistics (European Meeting Statisticians, Budapest, 1972)* (North-Holland, Amsterdam, 1974), p. 241.

[25] C. W. Gardiner *et al.*, *Handbook of Stochastic Methods* (Springer, Berlin, 1985), Vol. 3.

[26] G. A. Pavliotis, *Stochastic Processes and Applications. Diffusion Processes, the Fokker-Planck and Langevin Equations* (Springer-Verlag, New York, 2014).

[27] P. Gomme, J. Monetary Econ. **32**, 51 (1993).

[28] T. F. Cooley and E. C. Prescott, in *Frontiers of Business Cycle Research* (Princeton University Press, Princeton, NJ, 1995), pp. 1–38.

[29] P. Janssen and P. Heuberger, Ecol. Model. **83**, 55 (1995).

[30] M. Caraglio, F. Baldovin, and A. L. Stella, Sci. Rep. **6**, 31461 (2016).

[31] R. Carmona and S. Molchanov, Probab. Theory Relat. Fields **102**, 433 (1995).

[32] Y. V. Fyodorov and J.-P. Bouchaud, J. Phys. A: Math. Theor. **41**, 372001 (2008).

[33] Y. V. Fyodorov, P. Le Doussal, and A. Rosso, J. Stat. Mech. (2009) P10005.

[34] A. Zamolodchikov and A. Zamolodchikov, Lectures on Liouville Theory and Matrix Models (2007).

[35] Y. V. Fyodorov and J. P. Keating, Philos. Trans. R. Soc. London A **372**, 20120503 (2014).

[36] F. Cooper, A. Khare, and U. Sukhatme, Phys. Rep. **251**, 267 (1995).

[37] H. Risken, in *The Fokker-Planck Equation* (Springer, Berlin, 1984), pp. 63–95.

[38] P. Jung and H. Risken, Z. Phys. B: Condens. Matter **59**, 469 (1985).

[39] J. Cook and B. Derrida, J. Stat. Phys. **57**, 89 (1989).

[40] W. van Saarloos, Phys. Rev. A **37**, 211 (1988).

[41] E. N. Economou, *Green's Functions in Quantum Physics* (Springer, Berlin, 1984), Vol. 3.

[42] M. Bramson, *Convergence of Solutions of the Kolmogorov Equation to Traveling Waves* (American Mathematical Society, Baltimore, MD, 1983), Vol. 285.

[43] L. Schiff, *Quantum Mechanics*, International Series in Pure and Applied Physics (McGraw-Hill, New York, 1955).

[44] M. Yor, *Exponential Functionals of Brownian Motion and Related Processes* (Springer Science & Business Media, Berlin, 2012).

[45] R. W. Robinett, Eur. J. Phys. **31**, 1 (2009).

[46] J. R. P. Angel and P. G. H. Sandars, in *Proceedings of the Royal Society of London A: Mathematical, Physical and Engineering Sciences*, The Hyperfine Structure Stark Effect. I. Theory (The Royal Society, London, 1968), Vol. 305, pp. 125–138.

[47] G. Bastard, E. E. Mendez, L. L. Chang, and L. Esaki, Phys. Rev. B **28**, 3241 (1983).

[48] E. Merzbacher, *Quantum Mechanics* (Wiley, New York, 1970).

[49] C. M. Bender and S. A. Orszag, *Advanced Mathematical Methods for Scientists and Engineers I* (Springer Science & Business Media, Berlin, 1999).

[50] D. Sornette, *Critical Phenomena in Natural Sciences: Chaos, Fractals, Self-organization and Disorder: Concepts and Tools* (Springer Science & Business Media, Berlin, 2006).

[51] M. Newman, Proc. R. Soc. London B **263**, 1605 (1996).

[52] T. Mora and W. Bialek, J. Stat. Phys. **144**, 268 (2011).

[53] T. Lukes and K. Somaratna, J. Phys. C: Solid State Phys. **2**, 586 (1969).

[54] B. Derrida, Phys. Rev. B **24**, 2613 (1981).

[55] J.-P. Bouchaud and M. Mézard, J. Phys. A: Math. Gen. **30**, 7997 (1997).

[56] R. Van Der Hofstad, W. König, and P. Mörters, Commun. Math. Phys. **267**, 307 (2006).

[57] J. Gärtner and W. König, in *Interacting Stochastic Systems* (Springer, Berlin, 2005), pp. 153–179.

[58] W. Lutz, B. C. O'Neill, and S. Scherbov, Science **299**, 1991 (2003).